ELSEVIER

Engineering Structures 22 (2000) 1690–1698

ENGINEERING STRUCTURES

www.elsevier.com/locate/engstruct

Quadrilateral shear panel

Pierre C.J. Hoogenboom [a,*], Johan Blaauwendraad [b]

[a] University of Tokyo, Concrete Laboratory, 7-3-1 Hongo Bunkyo-ku, Tokyo 113-8565, Japan
[b] Delft University of Technology, Department of Civil Engineering, P.O. Box 5048, 2600 GA Delft, The Netherlands

Received 5 February 1999; received in revised form 21 May 1999; accepted 18 June 1999

Abstract

Various models of structures and structural elements use an assembly of stringers and shear panels. The normal forces in the stringers can vary linearly and the membrane panels have constant shear. Often, these shear panels can be just rectangular but sometimes shear panels with a non-rectangular shape need to be used. In this paper a mathematical formulation is presented for a linear–elastic shear panel with a quadrilateral shape. The panel stiffness matrix is derived by the discrete element method, which yields a simple and efficient computational formulation. Comparison with finite element computations shows that the stiffness matrix is sufficiently accurate for engineering design. © 2000 Elsevier Science Ltd. All rights reserved.

Keywords: Shear panel; Stringer–panel model; Discrete element method; Shear wall; Diaphragm; Membrane; Disk

1. Introduction

The structural behaviour of plates loaded in their plane often can be described using a discrete element model [1] consisting of stringers and shear panels. The normal forces in these stringer elements can vary linearly and the membrane panel elements have constant shear. For example, models of aircraft wings and aircraft fuselages [2], walls and floors of timber houses [3], metal plate girders [4] and joints, reinforced concrete walls (see Fig. 1) [5–7] and framed–tube structures of high-rise buildings [8,9]. Normally, these models use rectangular shear panels. The stiffness matrix of such a panel is well known and can be easily derived [10]. Some structures have a tapered shape or non-rectangular holes. To this end, parallelogramic and trapezoidal shear panels have been derived [2]. Formulations for quadrilateral shear panels were already proposed in 1951 [11] and also recently [12,13]. Obviously, this further extends the potential application of shear panels and removes restrictions for drafting panel assemblies in a graphical user-interface. However, these formulations appear to be accurate only if the shape of the quadrilateral panel does not depart too far from a rectangle. This paper contributes to the development by presenting a simple mathematical formulation for a linear–elastic shear panel of quadrilateral shape and comparing this and previous formulations with accurate finite element computations.

The panel has four edge tractions (see Fig. 2) and three independent equilibrium relations (in x direction, in y direction and moment equilibrium). Consequently, only one independent parameter β is available to describe the stress field. It will be shown that each traction is accompanied by a discrete edge displacement (see Fig. 2). So, the panel has four degrees of freedom too. Since it has three independent rigid body motions (two translations and one rotation) only one generalised displacement e is left to describe its deformation. The relations are displayed in Fig. 3.

Since linear–elastic material behaviour is adopted, the panel stiffness matrix $\boldsymbol{K}$ relates the vector with panel forces $\boldsymbol{f}$ to the discrete displacement vector $\boldsymbol{u}$.

$$\boldsymbol{f} = \boldsymbol{K}\boldsymbol{u} \tag{1}$$

As common in the discrete element method we assume that the stiffness matrix can be de-composed as

$$\boldsymbol{K} = \boldsymbol{B}^{\mathrm{T}}\boldsymbol{D}\boldsymbol{B} \tag{2}$$

In the next section the equilibrium vector $\boldsymbol{B}^{\mathrm{T}}$ is

* Corresponding author.
E-mail addresses: hgb@concrete.t.u-tokyo.ac.jp (P.C.J. Hoogenboom), j.blaauwendraad@ct.tudelft.nl (J. Blaauwendraad).

PII: S0141-0296(99)00061-9

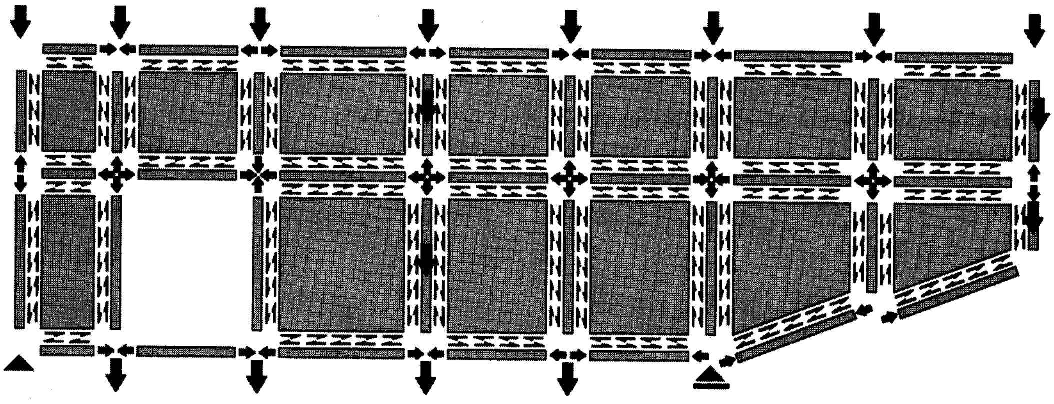

Fig. 1. A model of a reinforced concrete deep beam consisting of stringers and panels. The stringers represent concrete parts with concentrated reinforcement and the shear panels represent concrete parts with distributed reinforcement.

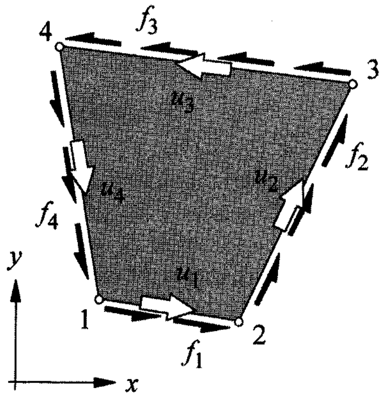

Fig. 2. The quadrilateral shear panel with a force f and a discrete displacement u at each edge.

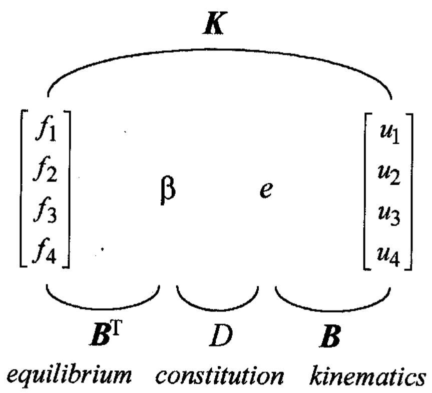

Fig. 3. The relations of the panel formulation according to the discrete element method. After applying equilibrium and kinematic requirements, only one relation is left to formulate the constitutive behaviour.

derived, which relates the edge forces f_1, f_2, f_3, f_4 and the generalised stress β (see Fig. 3). In Section 3, it is shown that this vector also defines the kinematic relation, which relates the generalised strain e and the discrete edge displacements u_1, u_2, u_3 and u_4. In Section 4, the constitutive relation is derived between the gener-

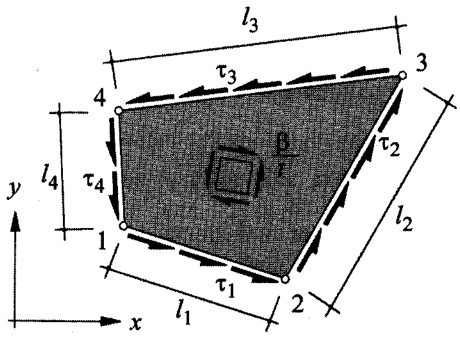

Fig. 4. The edge tractions on a quadrilateral shear panel. Obviously, the forces must be in equilibrium.

alised strain e and the generalised stress β. In Section 5 and Section 6 the derived formulation is tested and in Section 7 a practical application is shown. In Appendix A the computer code is included for efficient computation of the panel stiffness matrix.

Opposite to what is mentioned in literature [12], a quadrilateral shear panel with uniform shear tractions can fulfil all equations of elasticity theory. Of course the field quantities are not homogeneous, and only in the points of the vertices, the stress field becomes singular. However, an exact closed-form solution has not been derived as yet and as a consequence well-chosen approximations have to be utilised in this paper. All derivations are performed in a two-dimensional Cartesian reference frame. It is noted that a three-dimensional treatment would not be successful because a shear panel curved out of plane is only in equilibrium when all shear tractions equal zero (unless loaded transversely).

2. Equilibrium relation

As drawn in Fig. 4, the quadrilateral panel is freely positioned in a two-dimensional Cartesian reference frame. The panel vertices are numbered 1 to 4 counterclockwise. At each edge a constant shear stress τ_1, τ_2, τ_3,

τ_4 is present. The positive direction of the edge stresses follows the vertex numbers. This specific layout can be easily implemented in a computer program.

The panel forces have to be in equilibrium in the x direction and y direction.

$$\begin{aligned}0 &= \tau_1 t l_1 \cos(\boldsymbol{x},\boldsymbol{v}_{12}) + \tau_2 t l_2 \cos(\boldsymbol{x},\boldsymbol{v}_{23}) \\ &+ \tau_3 t l_3 \cos(\boldsymbol{x},\boldsymbol{v}_{34}) + \tau_4 t l_4 \cos(\boldsymbol{x},\boldsymbol{v}_{41}) \\ 0 &= \tau_1 t l_1 \sin(\boldsymbol{x},\boldsymbol{v}_{12}) + \tau_2 t l_2 \sin(\boldsymbol{x},\boldsymbol{v}_{23}) \\ &+ \tau_3 t l_3 \sin(\boldsymbol{x},\boldsymbol{v}_{34}) + \tau_4 t l_4 \sin(\boldsymbol{x},\boldsymbol{v}_{41})\end{aligned} \tag{3}$$

The notation $\cos(\boldsymbol{x},\boldsymbol{v}_{12})$ represents the cosine of the angle of the x-axis and the vector from vertex 1 to vertex 2. The panel thickness is denoted t and the lengths of the edges are l_1, l_2, l_3 and l_4 as shown in Fig. 4.

Moment equilibrium yields the following equation.

$$\begin{aligned}0 = &-\tau_1 t l_1 \cos(\boldsymbol{x},\boldsymbol{v}_{12}) y_1 + \tau_1 t l_1 \sin(\boldsymbol{x},\boldsymbol{v}_{12}) x_1 \\ &- \tau_2 t l_2 \cos(\boldsymbol{x},\boldsymbol{v}_{23}) y_2 + \tau_2 t l_2 \sin(\boldsymbol{x},\boldsymbol{v}_{23}) x_2 \\ &- \tau_3 t l_3 \cos(\boldsymbol{x},\boldsymbol{v}_{34}) y_3 + \tau_3 t l_3 \sin(\boldsymbol{x},\boldsymbol{v}_{34}) x_3 \\ &- \tau_4 t l_4 \cos(\boldsymbol{x},\boldsymbol{v}_{41}) y_4 + \tau_4 t l_4 \sin(\boldsymbol{x},\boldsymbol{v}_{41}) x_4\end{aligned} \tag{4}$$

Expressing the cosines and sines in the vertex co-ordinates,

$$\begin{aligned}\cos(\boldsymbol{x},\boldsymbol{v}_{12}) &= \frac{x_2 - x_1}{l_1} & \sin(\boldsymbol{x},\boldsymbol{v}_{12}) &= \frac{y_2 - y_1}{l_1} \\ \cos(\boldsymbol{x},\boldsymbol{v}_{23}) &= \frac{x_3 - x_2}{l_2} & \sin(\boldsymbol{x},\boldsymbol{v}_{23}) &= \frac{y_3 - y_2}{l_2} \\ \cos(\boldsymbol{x},\boldsymbol{v}_{34}) &= \frac{x_4 - x_3}{l_3} & \sin(\boldsymbol{x},\boldsymbol{v}_{34}) &= \frac{y_4 - y_3}{l_3} \\ \cos(\boldsymbol{x},\boldsymbol{v}_{41}) &= \frac{x_1 - x_4}{l_4} & \sin(\boldsymbol{x},\boldsymbol{v}_{41}) &= \frac{y_1 - y_4}{l_4}\end{aligned} \tag{5}$$

the equilibrium equations can be simplified:

$$\begin{aligned}0 &= \tau_1(x_2 - x_1) + \tau_2(x_3 - x_2) + \tau_3(x_4 - x_3) + \tau_4(x_1 - x_4) \quad 0 = \tau_1(y_2 - y_1) + \tau_2(y_3 - y_2) \\ &+ \tau_3(y_4 - y_3) + \tau_4(y_1 - y_4) \quad 0 = \tau_1(x_1 y_2 - x_2 y_1) + \tau_2(x_2 y_3 - x_3 y_2) + \tau_3(x_3 y_4 - x_4 y_3) \\ &+ \tau_4(x_4 y_1 - x_1 y_4)\end{aligned} \tag{6}$$

The generalised stress β is defined as the average of the stresses at the panel edges times the panel thickness t. This average shear flow can be interpreted as an approximation of the panel shear forces in the middle of the panel as close as possible in the direction of the edges (see Fig. 4).

$$\beta = \frac{1}{4}(-\tau_1 + \tau_2 - \tau_3 + \tau_4)t \tag{7}$$

The four previous equations can be written in matrix notation,

$$\begin{bmatrix} c_1 & c_2 & c_3 & c_4 \\ s_1 & s_2 & s_3 & s_4 \\ r_1 & r_2 & r_3 & r_4 \\ -1 & 1 & -1 & 1 \end{bmatrix} \begin{bmatrix} \tau_1 \\ \tau_2 \\ \tau_3 \\ \tau_4 \end{bmatrix} = \begin{bmatrix} 0 \\ 0 \\ 0 \\ 4\beta/t \end{bmatrix} \tag{8}$$

where the elements are defined according to

$$\begin{aligned}&c_1 = x_2 - x_1 \quad c_2 = x_3 - x_2 \quad c_3 = x_4 - x_3 \quad c_4 = x_1 - x_4 \\ &s_1 = y_2 - y_1 \quad s_2 = y_3 - y_2 \quad s_3 = y_4 - y_3 \quad s_4 = y_1 - y_4 \\ &r_1 = x_1 y_2 - x_2 y_1 \quad r_2 = x_2 y_3 - x_3 y_2 \quad r_3 = x_3 y_4 - x_4 y_3 \quad r_4 = x_4 y_1 - x_1 y_4\end{aligned} \tag{9}$$

Using Cramers rule τ_1 can be solved,

$$\tau_1 = \frac{\begin{vmatrix} 0 & c_2 & c_3 & c_4 \\ 0 & s_2 & s_3 & s_4 \\ 0 & r_2 & r_3 & r_4 \\ 4\beta/t & 1 & -1 & 1 \end{vmatrix}}{\begin{vmatrix} c_1 & c_2 & c_3 & c_4 \\ s_1 & s_2 & s_3 & s_4 \\ r_1 & r_2 & r_3 & r_4 \\ -1 & 1 & -1 & 1 \end{vmatrix}} = \frac{-\dfrac{4\beta}{t}\begin{vmatrix} c_2 & c_3 & c_4 \\ s_2 & s_3 & s_4 \\ r_2 & r_3 & r_4 \end{vmatrix}}{\begin{vmatrix} c_2 & c_3 & c_4 \\ s_2 & s_3 & s_4 \\ r_2 & r_3 & r_4 \end{vmatrix} + \begin{vmatrix} c_1 & c_3 & c_4 \\ s_1 & s_3 & s_4 \\ r_1 & r_3 & r_4 \end{vmatrix} + \begin{vmatrix} c_1 & c_2 & c_4 \\ s_1 & s_2 & s_4 \\ r_1 & r_2 & r_4 \end{vmatrix} + \begin{vmatrix} c_1 & c_2 & c_3 \\ s_1 & s_2 & s_3 \\ r_1 & r_2 & r_3 \end{vmatrix}} \tag{10}$$

where the numerator is expanded to the first column and the denominator to the bottom row. With the notation for the minors

$$k_1 = \begin{vmatrix} c_2 & c_3 & c_4 \\ s_2 & s_3 & s_4 \\ r_2 & r_3 & r_4 \end{vmatrix} \quad k_2 = \begin{vmatrix} c_1 & c_3 & c_4 \\ s_1 & s_3 & s_4 \\ r_1 & r_3 & r_4 \end{vmatrix} \quad k_3 = \begin{vmatrix} c_1 & c_2 & c_4 \\ s_1 & s_2 & s_4 \\ r_1 & r_2 & r_4 \end{vmatrix} \quad k_4 = \begin{vmatrix} c_1 & c_2 & c_3 \\ s_1 & s_2 & s_3 \\ r_1 & r_2 & r_3 \end{vmatrix} \tag{11}$$

and $f_1 = l_1 \tau_1 t$ this can be conveniently written as

$$f_1 = \frac{-4 k_1 l_1 \beta}{k_1 + k_2 + k_3 + k_4} \tag{12}$$

It can be shown that the minors are invariant of the position and orientation of the reference frame. Similar expressions can be derived for f_2, f_3 and f_4,

$$f_2 = \frac{4k_2l_2\beta}{k_1+k_2+k_3+k_4} \quad f_3 = \frac{-4k_3l_3\beta}{k_1+k_2+k_3+k_4} \tag{13}$$

$$f_4 = \frac{4k_4l_4\beta}{k_1+k_2+k_3+k_4}$$

From this the definition of vector $\boldsymbol{B}^{\mathrm{T}}$ follows:

$$f = \boldsymbol{B}^{\mathrm{T}}\boldsymbol{\beta} \qquad \boldsymbol{B}^{\mathrm{T}} = \frac{4}{k_1+k_2+k_3+k_4}\begin{bmatrix} -k_1l_1 \\ k_2l_2 \\ -k_3l_3 \\ k_4l_4 \end{bmatrix} \tag{14}$$

Thus, the equilibrium relation is derived.

3. Kinematic relation

In this section the kinematic relation between the generalised strain e and the discrete displacements u_1, u_2, u_3 and u_4 is derived. A derivation with complementary potential energy is used because it is possible to estimate the stress field due to the simple load and geometry of a shear panel. The total complementary potential energy Π_c in the panel is

$$\Pi_c = t\int_A \Pi_c'\,\mathrm{d}A - t\int_{l_1}\tau_1u_l'\,\mathrm{d}l_1 - t\int_{l_2}\tau_2u_2'\,\mathrm{d}l_2 - t\int_{l_3}\tau_3u_3'\,\mathrm{d}l_3 - t\int_{l_4}\tau_4u_4'\,\mathrm{d}l_4 \tag{15}$$

where t is the panel thickness, Π_c' is the local complementary potential energy per volume and A is the panel surface area. In general, the displacement components in the direction of the edges u_1',u_2',u_3',u_4' are a function of the position along their edges l_1, l_2, l_3, l_4. The shear tractions τ_1, τ_2, τ_3, τ_4 at the edges are defined constant. It is assumed that an edge displacement varies linearly along its edge so that the equation can be simplified.[1]

$$\Pi_c = t\int_A \Pi_c'\,\mathrm{d}A - t\tau_1u_1l_1 - t\tau_2u_2l_2 - t\tau_3u_3l_3 - t\tau_4u_4l_4 \tag{16}$$

where u_1, u_2, u_3, u_4 are the discrete displacements of the edge middles in the direction of the edges. Substituting the shear tractions $\tau_1 = f_1/(tl_1)$, $\tau_2 = f_2/(tl_2)$, $\tau_3 = f_3/(tl_3)$, $\tau_4 = f_4/(tl_4)$ and Eq. (14) in Eq. (16) gives the following result

$$\Pi_c = t\int_A \Pi_c'\,\mathrm{d}A - e\beta \tag{17}$$

where the generalised strain e is defined with the kinematic relation as

$$e = \boldsymbol{Bu} \tag{18}$$

4. Constitutive relation

Among all statically admissible stress fields, the actual one minimises the complementary potential energy. So

$$\frac{\mathrm{d}}{\mathrm{d}\beta}\Pi_c = 0 \tag{19}$$

From Eqs. (17) and (19) the constitutive relation between the generalised stress β and the generalised strain e can be derived.

$$e = \frac{\mathrm{d}}{\mathrm{d}\beta}t\int_A \Pi_c'\,\mathrm{d}A \tag{20}$$

This simple relation confirms the proper choice of the kinematic relation Eq. (18). It is very similar to Castigliano's second rule.

The local complementary potential energy Π_c', of a plane stress field in a linear–elastic material is

$$\Pi_c' = \frac{1}{2}\sigma_{xx}\varepsilon_{xx} + \frac{1}{2}\sigma_{yy}\varepsilon_{yy} + \frac{1}{2}\sigma_{xy}\gamma_{xy} \tag{21}$$

where σ_{xx}, σ_{yy} and σ_{xy} are the normal stresses and shear stress. ε_{xx}, ε_{yy} and γ_{xy}, are the strains in the x and y-directions and the shear strain, respectively. In general, not only shear stresses exist in a quadrilateral shear panel but normal stresses as well. It was found that these normal stresses can contribute considerably to the panel deformation. The x and y directions for the local energy are perpendicular but not related to the global reference frame. For isotropic material the complementary potential energy evaluates to

$$\Pi_c' = \frac{\sigma_{xy}^2}{2G} + \frac{\sigma_{xx}^2 - 2\nu\sigma_{xx}\sigma_{yy} + \sigma_{yy}^2}{2E} \tag{22}$$

As Fig. 5 shows, the skew shear stress τ at a parallelogramic elementary part of a panel can be easily transferred to orthogonal directions. When these stresses are substituted in Eq. (22) the following result is obtained.

$$\Pi_c' = \frac{\tau^2}{2G^*} \qquad \frac{1}{G^*} = \frac{1}{G} + \frac{4\cot^2\alpha}{E} \tag{23}$$

[1] It is possible to interpret a discrete edge displacement as the average along the panel edge of the displacement component in the edge direction. In this way the approximation to arrive at Eq. (16) is not needed. However, the authors prefer to avoid average displacements because this concept is rather abstract for practical use and not necessary in this case.

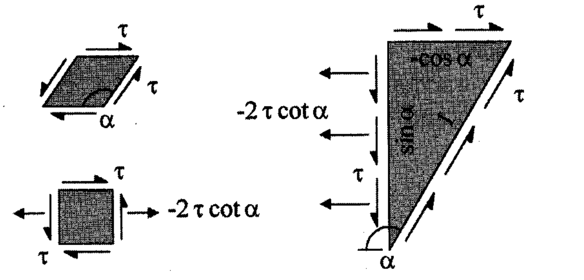

Fig. 5. The shear stresses in a skew reference frame can be easily transformed to orthogonal directions.

where α is the angle between the local skew directions as shown in Fig. 5. Note that the skew shear modulus G^* is a function of α. In Fig. 6, a general shear panel is drawn with a skew reference frame. It can be easily observed that each subdivision can be approximated with a parallelogramic element and that this approximation gets better when the subdivision becomes denser. It was observed from stress analyses on finite element models of shear panels that the normal stress in the skew reference frame remains small even for highly-nonrectangular panels. So, in the skew reference frame only shear stresses are assumed to exist.

According to Eq. (20), the local complementary potential energy in Eq. (23) should be integrated over the panel area.

$$e = t\int_A \frac{\mathrm{d}}{\mathrm{d}\beta}\frac{\tau^2}{2G^*}\,\mathrm{d}A \tag{24}$$

The integration can be transformed to the skew co-ordinates ξ and η (see Fig. 6)

$$e = t\int_{\eta=0}^{1}\int_{\xi=0}^{1} \frac{\mathrm{d}}{\mathrm{d}\beta}\frac{\tau^2}{2G^*}J\,\mathrm{d}\xi\,\mathrm{d}\eta \tag{25}$$

where J is the determinant of the Jacobian matrix.

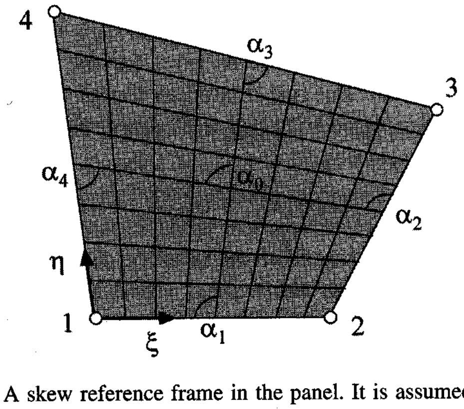

Fig. 6. A skew reference frame in the panel. It is assumed that only skew shear stresses occur in this reference frame. The points at the middles of the edges are used for approximation of the complementary potential energy.

$$J = A + \left(\frac{1}{2}-\xi\right)(c_1s_3 - c_3s_1) + \left(\frac{1}{2}-\eta\right)(c_2s_4 - c_4s_2) \tag{26}$$

The cot α can be derived as

$$\cot\alpha = \frac{(\eta c_3 + (\eta-1)c_1)(\xi c_2 + (\xi-1)c_4) + (\eta s_3 + (\eta-1)s_1)(\xi s_2 + (\xi-1)s_4)}{(\eta s_3 + (\eta-1)s_1)(\xi c_2 + (\xi-1)c_4) - (\eta c_3 + (\eta-1)c_1)(\xi s_2 + (\xi-1)s_4)} \tag{27}$$

Eq. (25) is evaluated with numerical integration. Since the stress field τ is not known in the interior of the panel, it is not convenient to use Gauss integration. Instead, Newton–Côtes integration was selected with integration points at the middles of the edges. Table 1 shows the weights for the integration points and the stresses in the integration points, which are consistent with Eq. (14). Note in Table 1 that differentiation of τ_i^2 to β can be easily performed. Thus, the expression for e becomes

$$e \approx t\sum_{i=1}^{4}\frac{\mathrm{d}}{\mathrm{d}\beta}\frac{\tau_i^2}{2G_i^*}w_iJ_i \tag{28}$$

Finally, the constitutive equation is

$$D = \frac{\beta}{e} \tag{29}$$

5. Validation

The final check of the formulation is a comparison with dense finite element models as shown in the next section. However, the formulation can readily be checked using the following five properties that are inherent to the exact behaviour of linear–elastic discrete elements:

1. No strains for rigid body displacements
2. Equilibrium
3. Reciprocity
4. Independence of the reference frame

Table 1
The weights of the numerical integration and the shear stresses in the integration points

Integration point i	ξ	η	Weight w_i	Shear stress τ_i
1	$\frac{1}{2}$	0	$\frac{1}{4}$	$\frac{\beta}{t}\frac{4k_1}{k_1+k_2+k_3+k_4}$
2	1	$\frac{1}{2}$	$\frac{1}{4}$	$\frac{\beta}{t}\frac{4k_2}{k_1+k_2+k_3+k_4}$
3	$\frac{1}{2}$	1	$\frac{1}{4}$	$\frac{\beta}{t}\frac{4k_3}{k_1+k_2+k_3+k_4}$
4	0	$\frac{1}{2}$	$\frac{1}{4}$	$\frac{\beta}{t}\frac{4k_4}{k_1+k_2+k_3+k_4}$

5. Reduction to exact relations for special geometries

The panel correctly complies with property 1. It also complies with property 2, which is no surprise because this property is imposed in the previous derivation. Property 3 is equivalent to symmetry of the stiffness matrix. The stiffness matrix is indeed symmetric as can be easily observed from Eq. (2). Property 4 is also fulfilled, since the minors k, the edge lengths l and the angles α are invariant of the reference frame. In the remainder of this section it is shown that the derived panel formulation agrees with property 5, too.

A rectangular shear panel has a homogeneous stress field for which the stiffness matrix can be derived without approximations [10]. When the vertex co-ordinates of a rectangular panel with dimensions a and b are used in the relations of the quadrilateral panel, the minors reduce to

$$k_1 = \begin{vmatrix} 0 & -a & 0 \\ b & 0 & -b \\ \frac{1}{2}ab & \frac{1}{2}ab & \frac{1}{2}ab \end{vmatrix} \quad k_2 = \begin{vmatrix} a & -a & 0 \\ 0 & 0 & -b \\ \frac{1}{2}ab & \frac{1}{2}ab & \frac{1}{2}ab \end{vmatrix}$$
$$k_3 = \begin{vmatrix} a & 0 & 0 \\ 0 & b & -b \\ \frac{1}{2}ab & \frac{1}{2}ab & \frac{1}{2}ab \end{vmatrix} \quad k_4 = \begin{vmatrix} a & 0 & -a \\ 0 & b & 0 \\ \frac{1}{2}ab & \frac{1}{2}ab & \frac{1}{2}ab \end{vmatrix} \tag{30}$$

which are evaluated to

$$k_1 = k_2 = k_3 = k_4 = a^2b^2 \tag{31}$$

The α_i are all $\pi/2$ so, the cot α_i are all zero. The shear stress is homogeneous $\tau = \beta/t$ and the determinant of the Jacobian matrix reduces to panel area $J = ab$. Thus, the constitutive relation becomes

$$D = \frac{Gt}{ab} \tag{32}$$

The $\boldsymbol{B}$ vector becomes

$$\boldsymbol{B} = [-a \;\; b \;\; -a \;\; b] \tag{33}$$

and the resulting stiffness matrix is

$$\boldsymbol{K} = \boldsymbol{B}^{\mathrm{T}}D\boldsymbol{B} = Gt\begin{bmatrix} \frac{a}{b} & -1 & \frac{a}{b} & -1 \\ -1 & \frac{b}{a} & -1 & \frac{b}{a} \\ \frac{a}{b} & -1 & \frac{a}{b} & -1 \\ -1 & \frac{b}{a} & -1 & \frac{b}{a} \end{bmatrix} \tag{34}$$

This is indeed the stiffness matrix of a rectangular shear panel. So, when the quadrilateral panel becomes rectangular the stiffness matrix correctly reduces to the simple stiffness matrix of a rectangular panel. The same can be shown for a parallelogramic shear panel, for which also an exact solution exists.

6. Comparison

The accuracy of the derived stiffness matrix is determined by comparison with finite element computations for several panel geometries. The procedure for the finite element computations is straightforward: First, unit values are chosen for the generalised stress $\beta = 1$, panel thickness $t = 1$ and shear modulus $G = 1$. The elasticity modulus $E = 2.4$ is consistent with Poisson's ratio $\nu = 0.2$. The panel edge tractions are calculated by Eq. (14). Subsequently, the deformations are computed with a linear–elastic finite element model. Finally, the generalised strain e is calculated with the discrete displacements u at the middle of the edges according to Eq. (18). The finite element models for various shapes consisted of 100 linear elements with four nodes.

The results are displayed in Table 2. Column 4 presents the compliances computed with the finite element model. Column 5 and 6 show the compliances of panel formulations derived by Curtis [12] and Chen [13], respectively. The last column contains the compliances computed with the proposed relation. Below the compliances, the deviations from the finite element solution are printed. From the table it becomes clear that the proposed formulation is substantially more accurate for one single panel than previous derivations. The error becomes larger when the panel deviates more from a parallelogram but is still small for the proposed formulation.

The compliances of the formulations of Curtis and of Chen were obtained in the same way as the finite element results. The simple formulation of Chen needed to be supplemented with stiff bar elements at the edges to prevent hourglass modes. The stiff behaviour of this formulation is indirectly caused by neglecting normal stresses in the derivation. The formulation of Curtis shows to be rather stiff too. Perhaps the reason for this is that in this formulation shear traction is not constant along a panel edge.

Previous formulations have been validated with a beam model consisting of stringers and panels. This is rather unfortunate because the individual panel behaviour gets lost between that of the other elements. The results are not included here, but for that beam, the present formulation gives the same force distribution and approximately the same displacements as found by others [12,13].

Already in 1951, a study was made on the quadrilat-

Table 2
Comparison of the compliance of shear panel formulations with finite element computations

Shape		Co-ordinates	Minors	$\frac{e}{\beta}$ (FEM)	$\frac{e}{\beta}$ (Curtis)	$\frac{e}{\beta}$ (Chen)	$\frac{1}{D}$ Eq. (28)
1	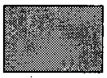	$(x_1 = 0, y_1 = 0)$	$k_1 = 36$				
		$(x_2 = 3, y_2 = 0)$	$k_2 = 36$	6.000	6.000	6.000	6.000
		$(x_3 = 3, y_3 = 2)$	$k_3 = 36$				
		$(x_4 = 0, y_4 = 2)$	$k_4 = 36$		0%	0%	0%
2	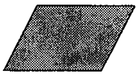	(0,0)	36				
		(3,0)	36	8.500	8.500	6.000	8.500
		(4,2)	36				
		(1,2)	36		0%	− 29%	0%
3	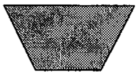	(1,0)	64				
		(3,0)	32	6.978	5.319	4.741	6.914
		(4,2)	16				
		(0,2)	32		− 24%	− 32%	− 1%
4	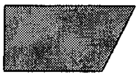	(0,0)	64				
		(3,0)	48	8.070	7.358	6.717	8.076
		(4,2)	36				
		(0,2)	48		− 9%	− 17%	0.1%
5	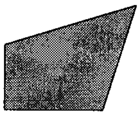	(0,0)	88				
		(3,0)	48	9.822	8.161	7.093	9.751
		(4,3)	54				
		(0,2)	99		− 17%	− 28%	− 1%
6	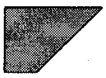	(0,0)	36				
		(1,0)	12	6.094	3.854	2.250	5.781
		(3,2)	4		− 37%	− 63%	− 5%
		(0,2)	12				

eral shear panel by Garvey, in which an essentially graphical method was used to obtain the stress distribution [11]. Garvey makes the same approximations as in this paper and derives a closed form expression for the complementary potential energy. Of course, at that time it was not possible to compare the formulation with accurate finite element computations.

It needs to be mentioned that the compliances of the finite element models depend somewhat on the definition of the degree of freedom. Here, it is assumed that the degrees of freedom are the displacements of the middles of the edges in the direction of the edges. However, it is also possible to define a degree of freedom as the average of the displacement along an edge. With this definition, the compliance of panel 3 becomes 6.501, which is approximately 7% stiffer than the result in Table 2. It was observed that this difference is related to normal stresses along the edges, which particularly occur in panel 3. Nevertheless, also for the alternative definition of the degrees of freedom, the accuracy of the proposed formulation will be often sufficient for engineering design.

7. Structural application

In the introduction to the paper, references are made to literature describing applications of shear panels. In order to further demonstrate the potential of shear panels an example is presented below. The large steel plate bracket (see Fig. 7) has an opening in the web and is loaded with a single force of 1000 kN. Stiffeners are welded at the edges of the opening and extended to the flanges. Fig. 8 shows the force flow in a stringer–panel model of the bracket. Stringer forces are displayed black in the case of tension and grey in the case of compression. The width of the displayed force is a measure for its value. The shear flow is plotted in the centres of the panels in N/mm. The linear–elastic stringer–panel model provides a simple yet sufficiently accurate way to quantify the forces for dimensioning of the bracket components. In comparison, a finite element model would require far more mouse-clicks to draw and generate an element mesh, especially if changes need to be made to the geometry in subsequent design cycles.

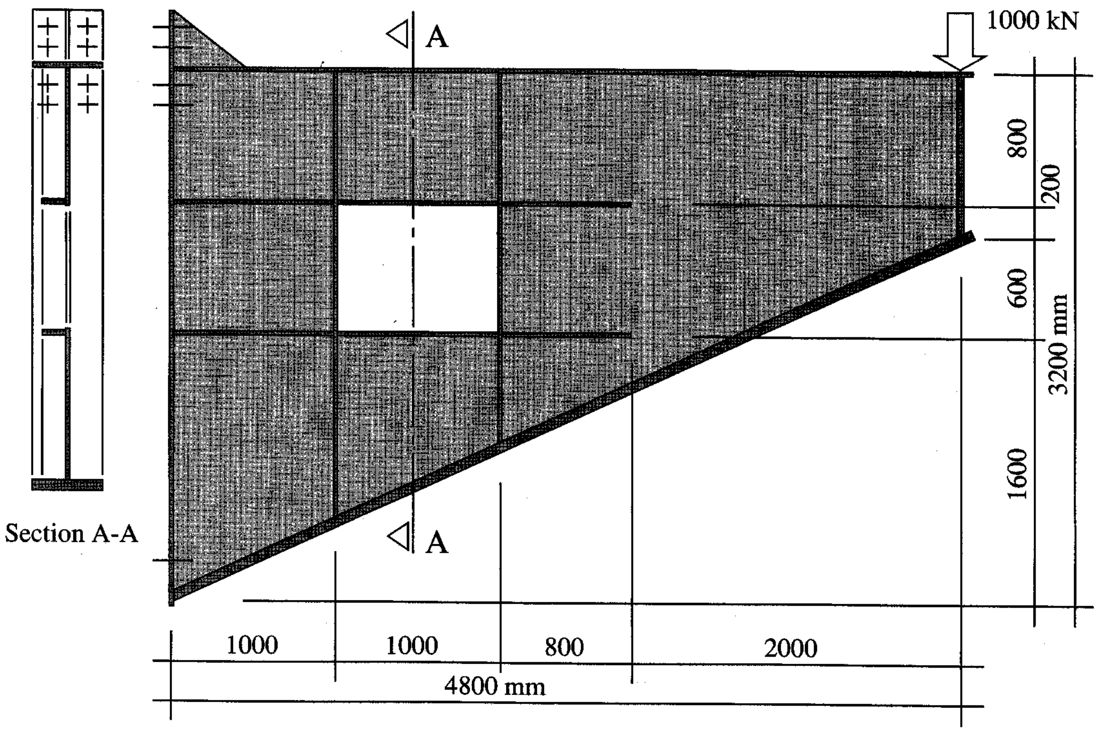

Fig. 7. A large steel plate bracket.

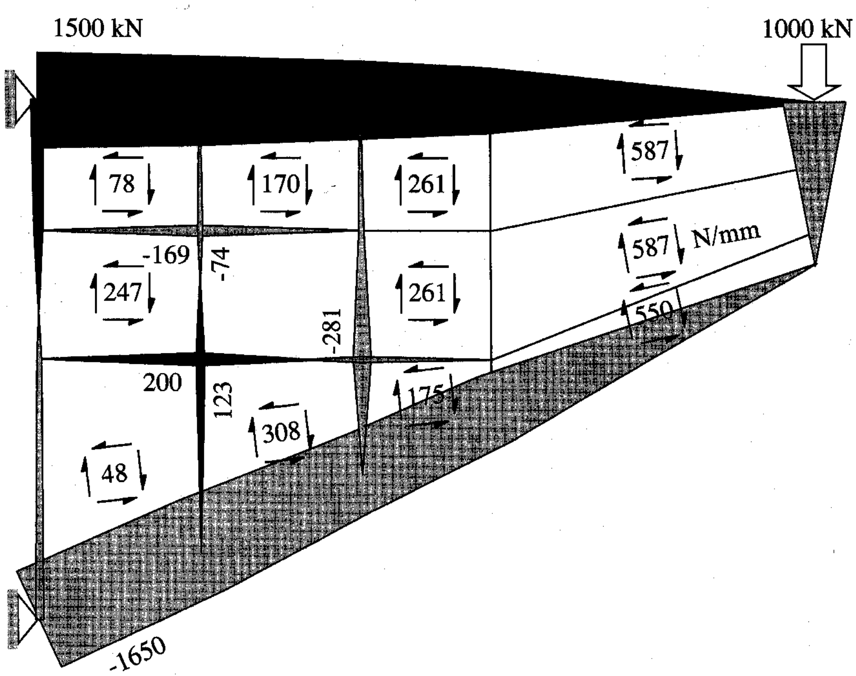

Fig. 8. The force flow in the stringer–panel model for the design load.

8. Conclusion

A mathematical formulation is presented of the linear–elastic behaviour of a quadrilateral shear panel. Despite its simplicity, the formulation appears to be more accurate than previously proposed formulations.

Acknowledgements

The authors wish to express their appreciation to H.A.B. te Lintelo for his contribution to the early versions of the quadrilateral shear panel and to Professor H.D. Curtis for his kind help in comparing the panel behaviours.

Appendix A. Computer Code

In order to show that the relations can be implemented efficiently, the PASCAL code is added for computation of the stiffness matrix of the proposed quadrilateral panel. Note that extra attention must be given to the computation of k_i^2 since it has the unit [length^8], which can produce an overflow of the number memory capacity if very small model units are chosen. The algorithm consists of only 69 additions or subtractions, 117 multiplications, 15 divisions and 4 square roots. The code uses 54 memory locations.

```
c1: = x2-x1; c2: = x3-x2; c3: = x4-x3; c4: = x1-x4;
s1: = y2-y1; s2: = y3-y2; s3: = y4-y3; s4: = y1-y4;
r1: = x1*y2-x2*y1; r2: = x2*y3-x3*y2; r3: = x3*y4-
x4*y3; r4: = x4*y1-x1*y4;
k1: = c2*(s3*r4-s4*r3)-s2*(c3*r4-c4*r3) + r2*(c3*
s4-c4*s3);
k2: = c1*(s3*r4-s4*r3)-s1*(c3*r4-c4*r3) + r1*(c3*
s4-c4*s3);
k3: = c1*(s2*r4-s4*r2)-s1*(c2*r4-c4*r2) + r1*(c2*
s4-c4*s2);
k4: = c1*(s2*r3-s3*r2)-s1*(c2*r3-c3*r2) + r1*(c2*
s3-c3*s2);
if (G > 0.0) and (E > 0.0) and (k1 > 0.0) and (k2 >
0.0) and (k3 > 0.0) and (k4 > 0.0) then begin
 l1: = sqrt(c1*c1 + s1*s1);
 l2: = sqrt(c2*c2 + s2*s2);
 l3: = sqrt(c3*c3 + s3*s3);
 l4: = sqrt(c4*c4 + s4*s4);
 A: = 0.50*(r1 + r2 + r3 + r4);
 k: = 0.25*(k1 + k2 + k3 + k4);
 B[1]: = -k1/k*l1; B[2]: = k2/k*l2;
 B[3]: = -k3/k*l3; B[4]: = k4/k*l4;
 t1: = c4-c2; t2: = s4-s2; t3: = c3-c1; t4: = s3-s1;
 g1: = (c1*t1 + s1*t2)/(s1*t1-c1*t2);
 g2: = (t3*c2 + t4*s2)/(t4*c2-t3*s2);
 g3: = (c3*t1 + s3*t2)/(s3*t1-c3*t2);
 g4: = (t3*c4 + t4*s4)/(t4*c4-t3*s4);
 t1: = 0.5*(c1*s3-c3*s1);
 t2: = 0.5*(c2*s4-c4*s2);
 j1: = A + t2; j2: = A-t1; j3: = A-t2; j4: = A + t1;
 t1: = 0.5/G; t2: = 2.0/E;
 p1: = t1 + t2*g1*g1; p2: = t1 + t2*g2*g2;
 p3: = t1 + t2*g3*g3; p4: = t1 + t2*g4*g4;
 h1: = k1/k; h1: = h1*h1;
 h2: = k2/k; h2: = h2*h2;
 h3: = k3/k; h3: = h3*h3;
 h4: = k4/k; h4: = h4*h4;
 s: = h1*p1*j1 + h2*p2*j2 + h3*p3*j3 + h4*p4*j4;
 D: = 2.0*t/s;
 for i: = 1 to 4 do for j: = 1 to 4 do K[i,j]: = B[i]*
 D*B[j];
end
else
 for i: = 1 to 4 do for j: = 1 to 4 do K[i,j]: = 0.0;
```

References

[1] El Naschie MS. Stress, Stability and Chaos in Structural Engineering, An Energy Approach. London: McGraw-Hill, 1990.
[2] Robinson J. Structural Matrix Analysis for the Engineer. New York: John Wiley & Sons, 1966.
[3] Kamiya F, Itani RY. Design of wood diaphragms with openings. Journal of Structural Engineering 1998;July:839–48.
[4] Davies AW, Roberts TM. Shear strength of welded aluminium alloy plate girders, structures and buildings. Institution of Civil Engineers 1998;128(3):308–14.
[5] Kder JC. The stringer method applied to discs with holes. Final Report IABSE Colloquium Plasticity in Reinforced Concrete, Copenhagen: IABSE, 1979:29.
[6] Nielsen MP. Limit Analysis and Concrete Plasticity. London: Prentice-Hall, 1984.
[7] Blaauwendraad J, Hoogenboom PCJ. Stringer panel model for structural concrete design. ACI Structural Journal 1996;93(3):295–305.
[8] Connor JJ, Pouangare CC. Simple model for design of framed–tube structures. Journal of Structural Engineering, ASCE 1991;117(12):3623–44.
[9] Jayachandran P, Browne MS. Approximate methods of analysis of tall framed–tube buildings. International Conference on Stability of Structures ICSS 95, June 7–9, Coimbatore (India), 1995:997–1008.
[10] Argyris JH, Kelsey S. Energy Theorems and Structural Analysis. London: Butterworths, 1960.
[11] Garvey SJ. The quadrilateral 'Shear' panel, the peculiar stressing problems arising in the structure of the non-rectangular swept wing. Aircraft Engineering 1951;23(267):134–5, 144.
[12] Curtis HD, Greiner GP. A stress-based quadrilateral shear panel. Finite Elements in Analysis and Design 1996;21:159–78.
[13] Chen HC. A simple quadrilateral shear panel element. Communications in Applied Numerical Methods 1992;8:1–7.